Hollow $CuSbS_y$ Coated by Nitrogen-Doped Carbon as Anode electrode for High Performance Potassium-Ion Storage

Ping Hu [1, ‡], Yulian Dong [2, ‡], Guowei Yang [1], Xin Chao [1], Shijiang He [1], Huaping Zhao [2], Qun Fu [1], and Yong Lei[2, *]

1. *Institute of Nanochemistry and Nanobiology, School of Environmental and Chemical Engineering, Shanghai University, Shanghai 200444, China.*
2. *Fachgebiet Angewandte Nanophysik, Institut für Physik & IMN MacroNano, Technische Universität Ilmenau, 98693 Ilmenau, Germany*

* Correspondence: yong.lei@tu-ilmenau.de

Instrumentation and Sample Analysis

Scanning electron microscopy (SEM, Nova nano F7500, FEI, USA) was used to observe the morphology of the materials. Energy dispersive spectroscopy (EDS, OXFORD Xplore, OXFORD Instruments) was used to measure the elemental distribution of the material at an accelerating voltage of 15 kV. Raman spectrometer (Raman, Renishaw Invia plus, Renishaw, UK) is used to characterize carbon materials. The transmission electron microscope (TEM, Tecnai G2 F20, FEI, USA) were employed to characterize the morphology and microstructure of the electrode materials. X-ray diffractometer (XRD, SmartLab, Rigaku, Japan) confirmed the crystal structure of the materials at a scanning speed of 10° min^{-1} with Cu Kα radiation (λ = 1.5406 Å). The chemical surface state and composition of the materials were characterized by X-ray photoelectron spectroscopy (XPS, Thermo Scientific K-Alpha, Waltham, MA, USA) with an Al Kα exciting source (hv= 1486.6 eV) and correct the C 1 s peak at 284.8 eV before sample analysis.

Electrochemical measurement

The anode was prepared by mixing $CuSbS_y$, Super-P, and CMC in distilled water in a 7:2:1 ratio to form a uniform slurry. The material was coated on copper foil with a scraper and dried in a vacuum at 60 ℃. A load of active materials on the copper foil was 1~2 mg/cm^2, which was measured by a microbalance of one part in ten thousand.

The button cell was assembled in an argon-filled glove box with a potassium plate as the counter electrode, the anode material separated from the potassium plate by a fiberglass film, and 2 M KFSI dissolved in EC/DEC as the electrolyte. Then, the constant current charging and discharging capacity of coulombic efficiency was measured by LAND at the voltage of 0.01~3 V. The GITT curve was also obtained by using the LAND test. The specific test procedure was as follows: (1) Let it stand for 10 h, and then discharge/charge it for 5 cycles; (2) Let it stand for 1 h to make the cycle reach equilibrium, and then continue the cycle discharge process, with the process time set to 9 mins, and cycle to the lower limit voltage (V≦0.01 V) in the discharge process; (3) Let it stand for another 1 h to make the cycle reach a balanced state, and then continue the cycle charging process, with the process time set to 9 mins, and cycle to the upper limit voltage (V≦3 V) in the charging process. An electrochemical workstation was used to perform electrochemical impedance spectroscopy and cyclic voltammograms. Nyquist plots were obtained by impedance testing using the VMP3 electrochemical workstation. The test software was EC-Lab. the test program was PEIS and the test frequency range was 100 kHz-10 mHz.

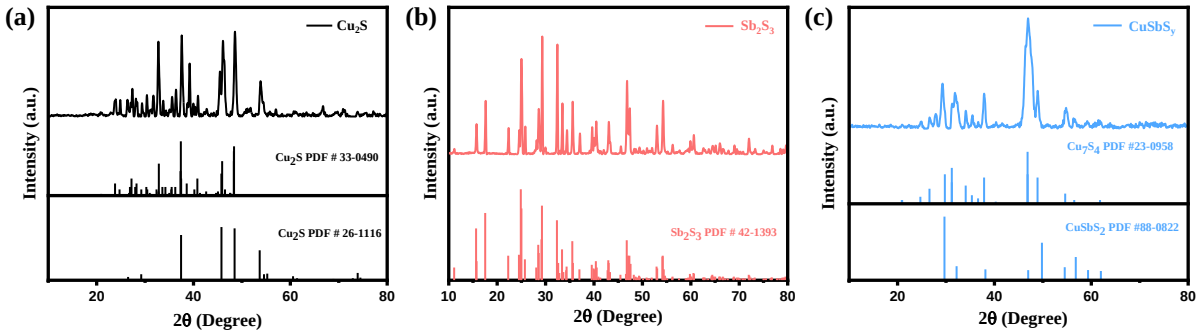

Figure S1. XRD patterns of (a) Cu_2S@C, (b) Sb_2S_3@C, (c) $CuSbS_y$.

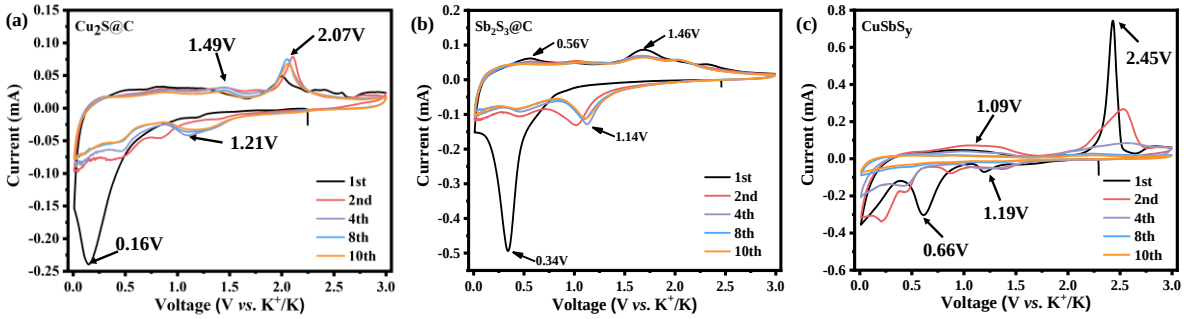

Figure S2. Initial ten CV curves of (a) Cu_2S@C, (b) Sb_2S_3@C, and (c) $CuSbS_y$ electrode at a scan rate of 0.1 mV s^{-1} in a potential range from 0.01-3 V.

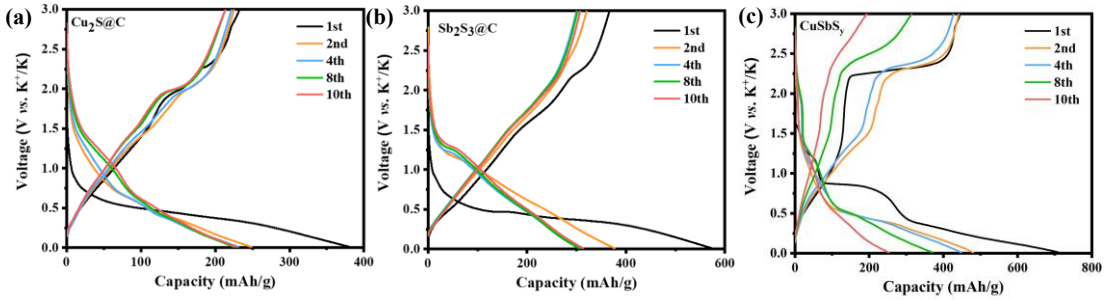

Figure S3. Charge/discharge profiles of (a) Cu_2S@C, (b) Sb_2S_3@C, and (c) $CuSbS_y$ electrodes within the potential of 0.01-3 V at a current density of 0.1 A g^{-1}.

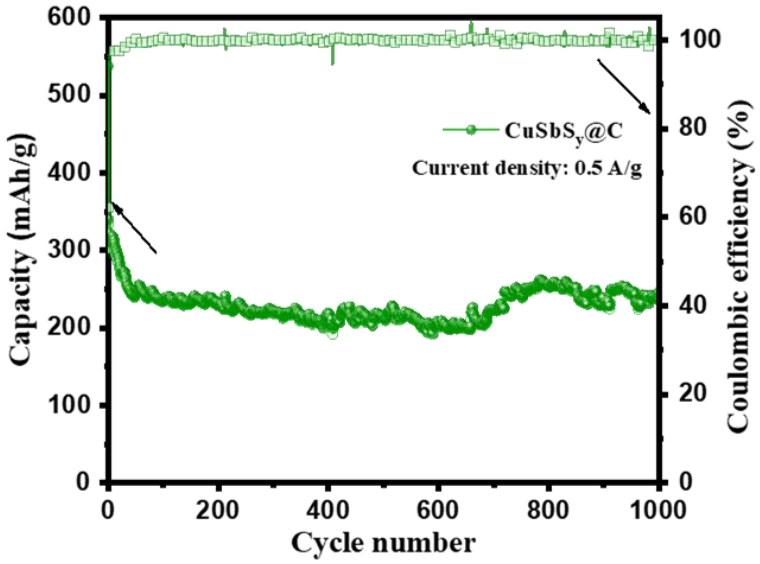

Figure S4. Cycling performance of $CuSbS_y$@C electrodes at current densities of 0.5 A g^{-1}.

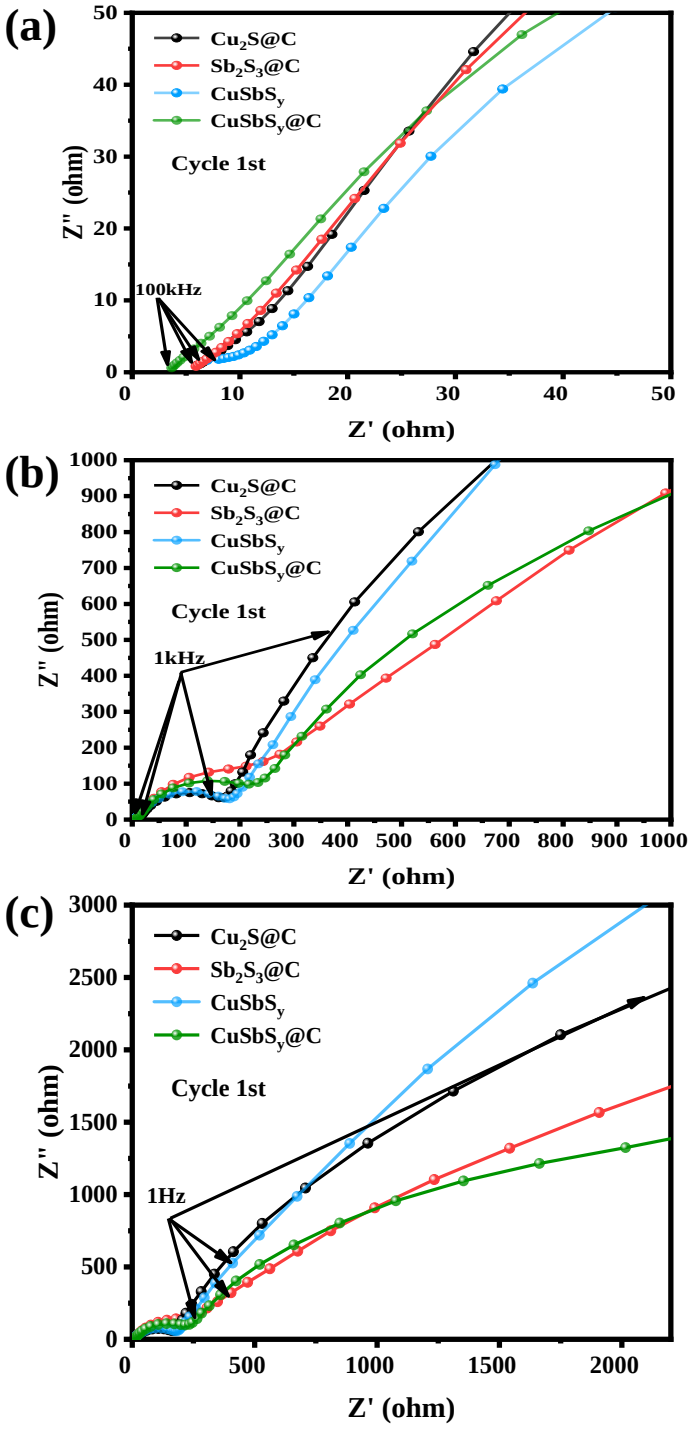

Figure S5. The positions of Cu_2S@C, Sb_2S_3@C, $CuSbS_y$, and $CuSbS_y$@C at (a) 100 kHz, (b) 1 kHz, and (c) 1 Hz.

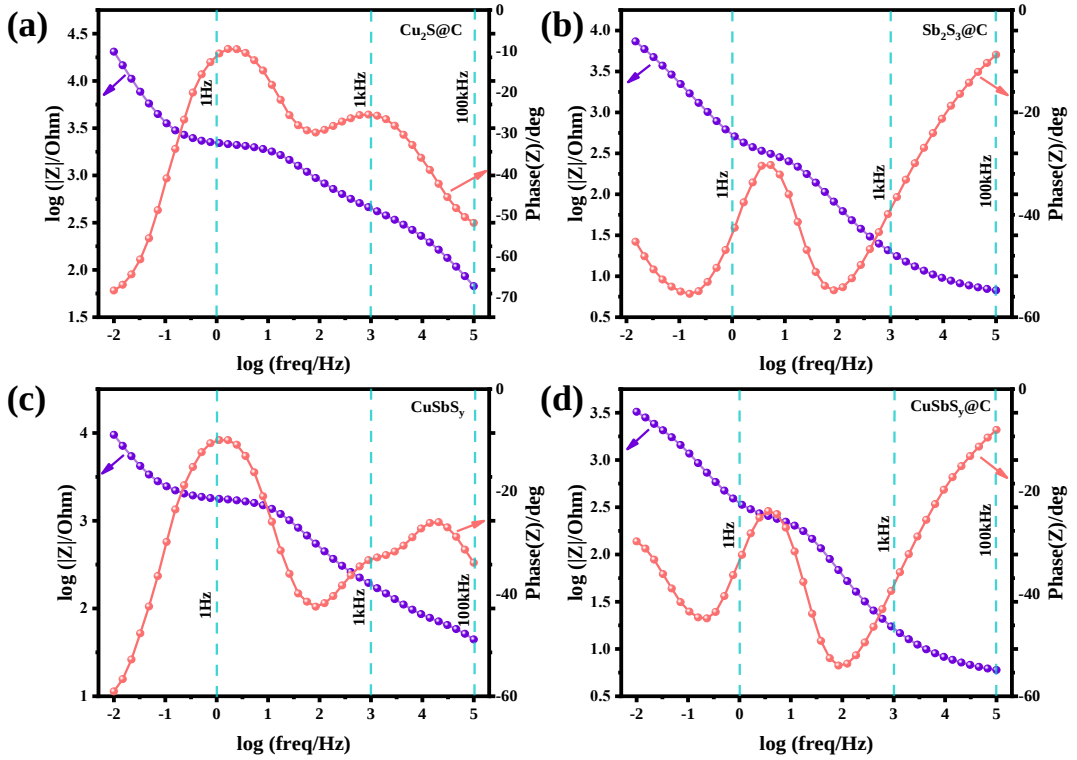

Figure S6. Bode plots of (a) Cu_2S@C, (b) Sb_2S_3@C, (c) $CuSbS_y$, and (d) $CuSbS_y$@C electrode.

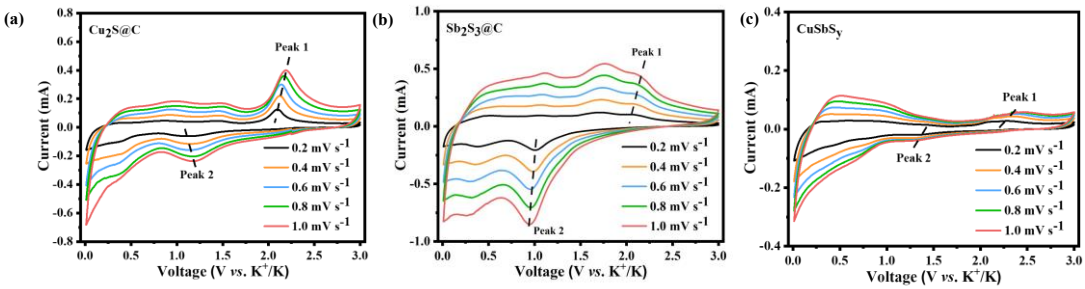

Figure S7. CV curves of (a) Cu_2S@C, (b) Sb_2S_3@C, and (c) $CuSbS_y$ electrode at various scan rates of 0.2-1.0 mV s^{-1}.

Table S1. Content of Cu, Sb, and S elements in the compounds.

	Cu	Sb	S
Content (%)	15.76	45.68	4.89

Table S2. Performance comparison between this study and existing studies.

Name	Electrolyte	Initial Coulomb efficiency	Cycle performance/ mAh g^{-1}	Rate capability/ mAh g^{-1}	Reference
$NiCo_2S_4$@N-HCNFs	0.8 M KPF_6 in EC:DEC	53.5%	263.7/0.1 A g^{-1}	117/3.2 A g^{-1}	[1]
$(Bi,Sb)_2S_3$	3 M KFSI in DME	~60%	611/0.1 A g^{-1}	302/0.8 A g^{-1}	[2]
$Co_1Sn_{6.75}$-S/rGO	1 M KFSI in DME	-	306.6/0.5 A g^{-1}	92.8/5 A g^{-1}	[3]
$FeCoS_2$@rGO	1 M KFSI in EMC	63.5%	365.2/0.1 A g^{-1}	182/2 A g^{-1}	[4]
CoS_2/ZnS@rGO	3M KFSI in EC/PC	63%	565/0.1 A g^{-1}	177.2/3 A g^{-1}	[5]
NiFeS@C	1 M KFSI in EC/DEC	53%	297/0.1 A g^{-1}	52/7 A g^{-1}	[6]
$CuSbS_y$@C	2 M KFSI in EC/DEC	66.9%	438.8/0.1 A g^{-1}	173.6/5 A g^{-1}	**This work**

Table S3. The comparison of R_s, R_{SEI}, and R_{ct} of Cu_2S@C, Sb_2S_3@C, $CuSbS_y$, and $CuSbS_y$@C.

		Cu_2S@C	Sb_2S_3@C	$CuSbS_y$	$CuSbS_y$@C
R_s (Ω)		6.951	6.007	9.285	5.173
R_{SEI} (Ω)		3.663	3.954	3.938	3.587
R_{ct} (Ω)	1 Cycle	146.9	252.1	153.4	211.0
	30 Cycles	445.6	383.4	664.2	315.2

Table S4. The comparison of τ_1, and τ_2 of Cu_2S@C, Sb_2S_3@C, $CuSbS_y$, and $CuSbS_y$@C.

	Cu_2S@C	Sb_2S_3@C	$CuSbS_y$	$CuSbS_y$@C
τ_1 (s)	0.00385	0.00448	0.0162	0.00571
τ_2 (s)	0.128	0.117	0.0177	0.227

1. Zhang, W.; Chen, J.; Liu, Y.; Liu, S.; Li, X.; Yang, K.; Li, L. Decoration of Hollow Nitrogen-Doped Carbon Nanofibers with Tapered Rod-Shaped $NiCo_2S_4$ as a 3D Structural High-Rate and Long-Lifespan Self-Supported Anode Material for Potassium-Ion Batteries. *J. Alloys Compd.* **2020**, *823*, 153631.
2. Wang, J.; Fan, L.; Liu, Z.; Chen, S.; Zhang, Q.; Wang, L.; Yang, H.; Yu, X.; Lu, B. In Situ alloying Strategy for Exceptional Potassium Ion Batteries *ACS Nano* **2019**, *13*, 3703-3713.
3. Chen, J.; Zhang, Y.; Chen, C.; Tian, N.; Zhang, Q.; Zhang, B. Graphene Wrapped Cobalt/Tin Bimetallic Sulfides Composites with Abundant Active Facets and Extended Interlayer Spacing for Stable Sodium/Potassium Storage *Chem. Eng. J.* **2022**, *442*, 136223.
4. Chen, X.; Cheng, N.; Zhang, L.; Xiang, G.; Ding, Y.-L.; Liu, Z. Flower-Like Spherical $FeCoS_2$ Coated by Reduced Graphene Oxide as Anode for High Performance Potassium Ion Storage. *J. Alloys Compd.* **2021**, *861*, 158458.
5. Iqbal, S.; Wang, L.; Kong, Z.; Zhai, Y.; Sun, X.; Wang, F.; Jing, Z.; He, X.; Dou, J.; Xu, L. In Situ Growth of CoS_2/ZnS Nanoparticles on Graphene Sheets as an Ultralong Cycling Stability *ACS Appl. Mater. Interfaces* **2022**, *14*, 15324-15336.
6. Yang, S.H.; Park, S.-K.; Park, G.D.; Kim, J.H.; Kang, Y.C. Rational Synthesis of Uniform Yolk–Shell Ni–Fe Bimetallic Sulfide Nanoflakes@Porous Carbon Nanospheres as Advanced Anodes for High-Performance Potassium-/Sodium-Ion Batteries. *Chem. Eng. J.* **2021**, *417*, 127963.